AIAA-99-0081
ACOUSTICS OF UNDER- AND OVER-EXPANDED COAXIAL JETS

Marco Debiasi* and Dimitri Papamoschou †
Department of Mechanical and Aerospace Engineering
University of California, Irvine
Irvine, CA 92697-3975

Abstract

Experiments have characterized the acoustics of axisymmetric high-speed jets at pressure-matched, over-expanded, and under-expanded conditions. The effect of an annular coflow on noise emission was also investigated. The fully-expanded jet velocity ranged from 430 m/s to 1010 m/s and the fully-expanded jet Mach number ranged from 1.25 to 1.75. The coflow was supplied at 200 m/s or 400 m/s, depending on the test case, and was designed for Mach wave elimination conditions. Noise spectra were obtained at many radial and polar positions around the jet exit. The peak noise emission in the far field is insensitive on nozzle exit pressure and depends solely on the values of the fully-expanded velocity and Mach number. In the lateral direction, imperfect expansion creates screech and broad-band shock noise. Addition of the coflow reduces the near-field screech peaks by 5-10 dB. The coflow suppressed Mach wave emission most effectively in jets with fully expanded velocity in the range of 600-700 m/s, providing reductions of as much as 18 dB in the mid- and high-frequency spectral components of the far field. Reduction of those spectral components was observed not only in the direction of peak emission but also in the lateral direction, where it ranged from 5 to 8 dB.

I. Introduction

The introduction of jet propulsion gave rise to the problem of jet noise suppression. Since the work of Westley and Lilley [1] on corrugated nozzles in the early 1950's, enormous effort has been devoted to quieting jet engines. These endeavors have been very successful in subsonic aircraft with the advent of high-bypass-ratio turbofan engines. Supersonic jet noise reduction, however, remains a vexing problem that has impeded the wide-scale development of supersonic air travel. The leading supersonic suppression scheme is the mixer-ejector [2, 3], a concept rooted also in the 1950's [4]. Its considerable noise benefits are unfortunately accompanied by appreciable thrust and weight penalties.

Supersonic jet noise consists of three main components: turbulent mixing noise, screech tones, and broadband shock noise, the latter two occurring in imperfectly expanded jets. At high speed, mixing noise is dominated by Mach wave emission which arises when turbulent eddies in the jet travel with a velocity which is supersonic relative to the surrounding medium. Mach wave radiation has been the subject of numerous analytical, computational, and experimental investigations. See for example references [5], [6], [7], [8], [9], and [10]. There is wide agreement that Mach wave emission is a phenomenon associated with a supersonic instability wave. It is radiated in the downstream direction. Reducing Mach wave emission is a key challenge for making high-speed transports environmentally acceptable [11]. In addition, Mach wave radiation can induce sonic fatigue of aircraft structures [12], so its near-field suppression is also important.

Screech is a discrete tone emitted by imperfectly-expanded jets. It has a significant upstream propagation component and thus can cause damage to the engine nozzle structure [13]. Screech is thought to be generated and sustained by a resonant feedback loop that comprises the following elements: (a) sound generated by passage of eddies through shock cells; (b) upstream propagation of the sound towards the nozzle; and (c) coupling of the sound with the shear-layer instability [14, 15, 16].

Recently, it was demonstrated that addition of an annular coflow to a supersonic jet can reduce noise if the convective velocity of the jet eddies with respect to the coflow drops to subsonic values, ensuring that the coflow eddies are also subsonic with respect to the ambient [17]. Letting M_{c_2} be the convective Mach num-

*Graduate Student, member AIAA
†Professor, member AIAA
0

ber of the eddies relative to the lower-velocity stream they are exposed to, the above requirements can be summarized as follows: M_{c_2} for both the jet and the coflow should be less than one. The concept is illustrated in Figs. 1 and 2. The method, called Mach wave elimination [18], achieved significant noise reductions in a pressure-matched jet with velocity of 920 m/s. It is now desired to test the method in a larger variety of jets exhausting at pressure-matched, over-expanded, and under-expanded conditions. We examine the effect of the coflow on Mach wave emission and screech noise.

II. Flow Conditions

Experiments were conducted in a coaxial jet facility detailed in [18]. Mixtures of helium and air were supplied to a concentric nozzle arrangement shown in Fig. 3. Subscripts 1,2, and ∞ refer to the jet, coflow, and ambient conditions respectively. The inner nozzles, of 12.7-mm exit diameter, were designed by the method of characteristics for Mach numbers $M_1 = 1.5$ and 1.75. The outer nozzle formed a smooth contraction terminating in an exit diameter of 25.4 mm. Precisely-metered mixtures of helium and air were supplied to the nozzles, which exhausted into ambient, still air. Helium-air mixtures simulate fairly accurately the density, velocity, and speed of sound of a heated jet. By regulating the mass fractions of helium and air, thereby regulating the gas constant of the mixture, we controlled the jet velocity at a given Mach number. The facility was equipped with pressure transducers which recorded the total pressures of the jet and coflow streams.

Table 1 summarizes the jet conditions covered in this study. Each jet is identified by a code, listed in the first column, which consists of a two-letter prefix (OE for over-expanded, PM for pressure-matched and UE for under-expanded) followed by the value of the fully-expanded velocity in m/s. The following three columns provide the nozzle-exit values of Mach number M_1, velocity U_1 and pressure ratio p_1/p_∞. The next two columns list the values of the fully (isentropically) expanded Mach number $M_{1\mathrm{fe}}$ and velocity $U_{1\mathrm{fe}}$. The last column indicates the calculated ratio of the thrust over the thrust of case PM920. The Reynolds number of the jet, based on its diameter D_1, ranged from a minimum of 380,000 in jet PM920 to a maximum of 740,000 in jet PM430.

Table 1 Jet conditions

Case	M_1	U_1	$\frac{p_1}{p_\infty}$	$M_{1\mathrm{fe}}$	$U_{1\mathrm{fe}}$	$\frac{F}{F_{\mathrm{PM920}}}$
OE430	1.50	480	0.72	1.28	430	0.70
PM430	1.50	430	1.00	1.50	430	0.96
OE630	1.50	700	0.71	1.27	630	0.71
PM630	1.50	630	1.00	1.50	630	1.01
OE700	1.75	770	0.68	1.50	700	0.92
PM700	1.50	700	1.00	1.50	700	0.98
OE820	1.50	920	0.70	1.25	820	0.73
OE920	1.75	1010	0.67	1.50	920	0.95
PM920	1.50	920	1.00	1.50	920	1.00
PM1010	1.75	1010	1.00	1.75	1010	1.52
UE1010	1.50	920	1.48	1.77	1010	1.55

U in m/s

Table 2 Coflow conditions

Case	M_2	U_2	$\frac{p_2}{p_\infty}$	$\frac{F}{F_{\mathrm{PM920}}}$
C200	0.60	200	1.00	0.45
C400	0.84	400	1.00	1.00

U in m/s

Table 2 summarizes the coflow properties. Each coflow is identified in the first column with the letter code C (for coflow) followed by the value of the coflow velocity in m/s. The following columns list the coflow Mach number M_2, velocity U_2 and pressure ratio p_2/p_∞. Since all the coflows were subsonic, their exit pressure was naturally matched to the ambient. The calculated ratio of the coflow thrust over the thrust of jet PM920 is provided in the last column. The coflow C200 was applied to the low-speed jets OE430 and PM430, while the coflow C400 was applied to the higher-speed jets. The intention was to keep the coflow velocity to within 40-65% of the jet velocity.

Coaxial jets (i.e. combinations of jet and coflow) are identified by a combination of the jet code and coflow code (e.g., PM920-C400). In this case, the coflow thrust ratio should be added to that of the jet to obtain the combined thrust ratio relative to reference case PM920. All the coaxial jets satisfy the Mach wave elimination criteria of [18]; however, some jets are safely inside the Mach wave elimination region while others are on its borderline.

III. Sound Measurement

For a detailed description of the sound instrumentation and signal processing procedures, the reader is referred

to [17]. It suffices here to state that the sound measurements were conducted inside the anechoic chamber a cutaway of which is shown in Fig. 4. The jet noise was recorded by a one-eighth inch condenser microphone (Bruel & Kjaer 4138) with a frequency response of up to 150 kHz. The microphone signal was sampled at 400 KHz. The power spectrum of each record (54280 points) was computed using a 512-point FFT with full Hanning window. The microphone was mounted on an arm which pivoted around an axis passing through the center of the jet exit as shown in Fig. 4. This arrangement enabled sound measurement at a variety of radial (r) and polar (θ) positions, r ranging from 0.038 to 1.52 m and θ ranging from 20^o to 100^o, measured counter-clockwise from the jet axis.

Central to our measurements is the spectrum of sound pressure level (SPL), obtained from

$$\text{SPL}(f) \;=\; 10\;\log_{10} S(f) \quad \text{(dB/Hz)}$$

where $S(f)$ is the power spectrum of $p'_{\text{rms}}/p_{\text{ref}}$, with p'_{rms} the root mean square pressure fluctuation and $p_{\text{ref}} = 20\ \mu$Pa the commonly used reference pressure. The power spectrum is corrected for the frequency and the free-field responses of the microphone, as explained in [17]. From the power spectrum, we also obtain the overall sound pressure level

$$\text{OASPL} \;=\; 10\;\log_{10} \int_0^{150\ \text{kHz}} S(f)df \quad \text{(dB)}$$

where the upper limit of the integration is dictated by highest frequency response of the microphone. Even though OASPL describes the total sound intensity at a given point, it is very inadequate as a measure of perceived noise. Sounds with same OASPL can have variations of up to 20 dB in perceived noise depending on their spectral content [4]. For this reason, we compute another important quantity which is the value of the SPL spectrum at $f = 100$ kHz, denoted $\text{SPL}_{\text{100-kHz}}$. Considering that our jet is 1/50 to 1/100 scale, a frequency of 100 kHz measured in our experiment corresponds to 1000-2000 Hz in a full-scale engine, i.e., the frequency range of maximum annoyance to humans. The 100-kHz component is defined here as the average spectral value of the bandwidth 100 ± 13 kHz and is computed as

$$\text{SPL}_{\text{100-kHz}} \;=\; 10\;\log_{10}\left[\frac{1}{\Delta f}\int_{f_0-\Delta f/2}^{f_0+\Delta f/2} S(f)df\right] \quad \text{(dB)}$$

with f_0=100 kHz and Δf =26 kHz.

All the noise measurements are scaled to equal thrust using standard geometric scaling procedures [17], with the thrust of jet PM920 used as a reference. The spectra are plotted versus the Strouhal number, $\text{St}=fD_1/U_1$ or $\text{St}=fD_{1\text{fe}}/U_{1\text{fe}}$ depending on the test case, where $D_{1\text{fe}}$ is the nozzle diameter required for perfect expansion. To relate our results to a full-scale engine with exit diameter of 1 m, the full-scale frequency is given approximately by

$$f_{\text{full-scale}} \;\approx\; \text{St}\; U_{1\text{fe}}$$

For velocities in the range of 700 m/s, the spectral components below St=0.3 correspond to $f_{\text{full-scale}} \leq$ 200 Hz, thus are not very significant to noise perceived by humans.

IV. Results

Effect of Imperfect Expansion

We first present the effect of nozzle exit pressure on the noise spectra in the direction of peak emission, which always occurred in the aft quadrant. We compare jets with same fully-expanded velocity and Mach number but different exit pressure ratios. The effect of coflow C400 on each of those jets is investigated. The comparison matrix is shown in Table 3, together with the results. The value of M_{c_2} shown in Table 3 is the convective mach number of the jet eddies with respect to their surrounding medium: ambient for single jets and coflow for coaxial jets. The value of M_{c_2} for coflow C400, with respect to ambient, is 0.70. The convective Mach number is calculated using the empirical shear-layer correlations of [19], recently refined for supersonic jets in [20].

Figure 5 presents the spectra of over-expanded and pressure-matched jets at same fully-expanded Mach number $M_{1\text{fe}} = 1.5$ and jet velocity $U_{1\text{fe}} = 700$ m/s (jets OE700 and PM700). Comparing the near-field spectra of Figs. 5(a) and (b), we see that over-expansion produces a screech tone at St=0.25. Application of the coflow removes the screech tone and reduces the spectrum by roughly 4 dB at St=0.25 and by about 20 dB for St>0.5. In the pressure-matched jet PM700, addition of the coflow produces similar high-frequency reductions but introduces a curious peak at very low frequency, St≈0.1. The reductions in the mid- and high-frequency spectral components is consistent with elimination of the Mach waves. The far-field spectra of cases OE700 and PM700, with and without coflow C400, are practically identical as shown in Figs. 5(c) and (d). With exception of the spectrum peak at St=0.1, the coflow reduces all the spectral components. For St>0.5, the reduction is around 12 dB.

Figure 6 compares under-expanded and pressure-matched jets at same fully-expanded Mach number $M_{1\text{fe}} \approx 1.75$ and jet velocity $U_{1\text{fe}} = 1010$ m/s (jets UE1010 and PM1010). Comparing Figs. 6(a) and 6(b) we notice that, not surprisingly, the near field of the under-expanded jet has a screech tone. As in the over-expanded case, the coflow eliminates the screech tone. Here, however, the coflow introduces a broad peak at very low frequencies, of roughly the same amplitude as the screech tone. A similar, but amplified peak is seen in the pressure-matched jet, Fig. 6(b). The near-field, high-frequency components are reduced by 12 dB in the under-expanded case and 20 dB in the pressure-matched case. The far-field spectra of Figs. 6(c) and (d) are very similar, indicating the insensitivity of the far-field noise on nozzle pressure. The coflow is ineffective here in reducing the noise, achieving a reduction of at most 3 dB. This is not so much the effect of under-expansion per se as it is the effect of the very high velocity and high Mach number of the jet, which result in a long Mach-wave emitting region which the coflow cannot cover completely. In addition, the jet convective Mach number M_{c_2} is 0.95, which is very borderline for Mach wave elimination.

The far-field results for these and other cases are summarized in Table 3. Clearly, the effect of nozzle pressure on peak sound emission is minimal. It is evident that the peak emission depends only of the values of the fully-expanded velocity and Mach number and that details of the very near field are immaterial. This correlates well with the recent finding of Tam [21] that nozzle shape has very small influence on far-field noise.

Table 3 Far-field noise at $r/D_1 = 80$ in the direction of peak emission

Case	$M_{1\text{fe}}$	$U_{1\text{fe}}$	M_{c_2}	OASPL	SPL at 100 kHz
OE700	1.50	700	1.77	132.57	67.24
PM700	1.50	700	1.76	132.67	68.04
OE700-C400	1.50	700	0.32	128.41	54.62
PM700-C400	1.50	700	0.32	129.71	55.13
OE920	1.50	920	2.14	133.98	69.92
PM920	1.50	920	2.12	134.96	69.93
OE920-C400	1.50	920	0.67	130.64	63.79
PM920-C400	1.50	920	0.66	130.09	62.91
PM1010	1.75	1010	2.53	135.08	71.31
UE1010	1.77	1010	2.54	136.14	70.41
PM1010-C400	1.75	1010	0.95	133.77	69.72
UE1010-C400	1.78	1010	0.95	134.37	67.84

OASPL and $\text{SPL}_{100\text{-kHz}}$ in dB

We now focus our attention in the lateral and slightly forward direction, $\theta = 100°$, where screech and broadband shock noise are supposed to be significant. To be consistent with earlier studies of these phenomena, we study the effects of imperfect expansion in jets with same exit velocity and Mach number. First, we examine over-expanded and pressure-matched jets with $M_1 = 1.5$ and $U_1 = 700$ m/s. Figure 7 presents the near and far fields of these jets, with and without coflow C400. Note that the frequency coordinate is now logarithmic to better depict the low-frequency spectral components. Comparing jets OE630 and PM700 in Figs. 7(a) and (b), we note that the near field of the over-expanded jet exhibits a pronounced peak at St=0.5, which is suppressed by the coflow. The coflow also reduces all the higher spectral components by 7-10 dB. The far field of the over-expanded case, shown in Fig 7(c), shows a series of small peaks near St=0.8, considerably higher than the frequency of the peak in the near field. The coflow suppresses those peaks and reduces the high-frequency components by 5-8 dB. The coflow seems less effective in reducing the far field spectrum of the pressure-matched case, seen in Fig. 7(d), and instead introduces a strange, broad peak at low frequency.

In Figure 8, we present the effect of under-expansion in the $\theta = 100°$ direction for jets with $M_1 = 1.5$ and $U_1 = 920$ m/s. Comparing the near fields, Figs. 8(a) and (b), and the far fields, Figs. 8(c) and (d), we note that under-expansion makes the spectrum very peaked. As we move from the near field to the far field, the peak shifts to higher frequency and its amplitude is reduced, a feature also seen in the over-expanded case above. The coflow is effective in reducing the near-field peak, Fig. 8(a), and the spectral components that follow it. In the far field, the coflow does not produce any spectacular changes.

Suppression of the screech tones by the coflow is probably a result of the coflow's ability to impede upstream propagation of signals that reach the nozzle lip of the jet. Thus, it interferes with the feedback loop which sustains screech. It is possible that a sonic or supersonic coflow will eliminate screech altogether.

There is good correlation of the reduction in the medium-to-high-frequency components measured in the $\theta = 100°$ direction with that measured in the direction of peak emission. Compare, for example, Fig. 5 to Fig. 7 and Fig. 6 to Fig. 8. Whenever the coflow produces appreciable noise reduction in the direction of peak emission, a similar benefit occurs in the lateral direction. Similarly, an ineffective coflow in one direction is also ineffective in the other direction. This suggests that Mach waves have an indirect effect on noise in the lateral direction, even though their propagation vector is in the downstream direction. This is not unexpected when one considers that each Mach wave is an envelope of spherical disturbances, the last of which (forming the tail end of the Mach wave) is cen-

tered at or near the nozzle exit and propagates in all directions. See for example the computations of Fenno et al. [12]. The higher the convective Mach number of the disturbance, the larger is their strength. Hence, reducing the convective Mach number by means of a coflow should bring noise reduction in all directions, not only in the direction of Mach wave emission.

Effect of M_{1fe} and U_{1fe} on Mach wave emission

We demonstrated above that the far-field peak noise emission depends solely on the fully-expanded values of Mach number and velocity. In this section we examine further the effect of those two parameters on Mach wave emission and Mach wave suppression by means of a coflow.

We begin by comparing the far-field spectra of jets with $M_{1fe} = 1.5$ and decreasing velocity U_{1fe}, shown in Fig. 9. The effect of coflows C400 on jets with $U_{1fe} \geq 630$ m/s and C200 on jets with $U_{1fe} < 630$ m/s is shown. The spectral peaks decline with decreasing U_{1fe}, although the drop is marginal at the higher velocities. The coflow is most effective in reducing the noise of jets with velocities of 630 m/s and 700 m/s, producing a drop of around 13 dB at the mid and high frequencies. Higher-speed jets have a long Mach-wave emitting region so this particular coflow, C400, has difficulty eliminating Mach waves far from the exit. In lower-speed jets, Mach waves are not as dominant a source of sound, so their elimination results in a smaller noise benefit.

Similar trends are seen in comparing spectra of jets with $M_{1fe} \approx 1.3$ and decreasing U_{1fe}, presented in Fig. 10. The maximum coflow benefit is observed at $U_{1fe} = 630$ m/s, where the spectrum is reduced by 18 dB for St>0.5. Evidently, decreasing the jet Mach number at fixed velocity reduces the Mach-wave emitting length of the jet, thereby enhancing the ability of the coflow to eliminate Mach waves.

Figures 11 and 12 summarize the results in terms of OASPL and $\mathrm{SPL}_{100\text{-kHz}}$, respectively, where the noise is plotted versus fully-expanded jet velocity for different fully-expanded jet Mach numbers. We note that both noise metrics increase rapidly with velocity at moderate velocities, but taper off at higher velocities. This is significant because it indicates that a reduction in jet velocity from 900 m/s to 700 m/s – via internal mixing of the core and bypass streams, for example – buys very marginal noise benefits, on the order 2-3 dB. The figures also illustrate that the peak far-field noise is virtually the same for over-expanded, pressure-matched, and under-expanded jets with the same M_{1fe} and U_{1fe}, consistent with our earlier observation. In terms of $\mathrm{SPL}_{100\text{-kHz}}$, the best noise reduction achieved with addition of the coflow occurs in the velocity range of 600-700 m/s and is 12 dB for $M_{1fe} = 1.5$ and 18 dB for $M_{1fe} \approx 1.3$. This reduction is plotted in Fig. 13 versus U_{1fe}. The fact that the noise benefit decreases for jet speeds less than 600 m/s, for which Mach wave emission is less dominant, indicates strongly that the primary action of the coflow is indeed Mach wave elimination versus reduction in the mean shear. The bypass ratios of the coaxial jets with best noise reduction were 1.7 for PM700-C400 and 2.4 for OE630-C400, values which are reasonable for a supersonic engine.

V. Concluding Remarks

The noise characteristics of perfectly and imperfectly expanded, low-density supersonic jets were studied with microphone surveys of the near and far fields. Application of a subsonic coflow at conditions designed to prevent emission of Mach waves from the jet was also investigated. This is a summary of the main conclusions:

(a) Peak noise emission in the far field is insensitive on the nozzle pressure ratio and depends solely on the values of the fully-expanded jet Mach number and velocity. This holds for both single and coaxial jets.

(b) In the direction of peak emission, application of the coflow reduces near-field and far-field spectra at all frequencies except the very low ones. Far-field noise reduction at St>0.5 was best for jet velocities in the range of 630-700 m/s, where reductions of up to 18 dB were measured.

(c) In the lateral direction, imperfectly expanded jets show distinctive screech tones in the near field, whose relative amplitude is reduced, and whose frequency is increased, in the far field. Addition of the coflow significantly attenuates the screech tones.

(d) Coflows that reduced the high-frequency components in the direction of peak emission were also effective in reducing such components in the lateral direction.

(e) Addition of a coflow to certain jets produced a broad, low-frequency spectral peak in the lateral direction. The origin of this peak is not understood. It may be tied to a specific nozzle geometry and needs to be further studied.

We did not yet have the opportunity to test the effect of the coflow on under-expanded jets with moderate and low speeds. Also, we did not optimize the coflow velocity and Mach number for a given jet configuration. It is hoped that such investigations will occur in the near future.

Acknowledgments

The support by NASA Lewis Research Center is gratefully acknowledged (Grant NAG-3-1981 monitored by Dr. Milo Dahl).

References

[1] Westley, R., and Lilley, G.M., "An Investigation of the Noise Field from a Small Jet and Methods for Its Reduction," College of Aeronautics, Rept. 53, Cranfield Univ., England, UK, Jan. 1952.

[2] Tillman, T.G., Paterson, R.W., and Presz, W.M., "Supersonic Nozzle Mixer Ejector," *AIAA Journal of Propulsion and Power*, Vol. 8, No. 2, 1992, pp. 513-519.

[3] Plencner, R.M., "Engine Technology Challenges for the High-Speed Civil Transport Plane," AIAA-98-2505.

[4] Smith, M.J.T., "Aicraft Noise," Cambridge University Press, Cambridge, 1989, pp. 9, 123.

[5] Tam, C.K.W. and Burton, D.E., "Sound Generated By Instability Waves of Supersonic Flows. Part 2. Axisymmetric Jets," *Journal of Fluid Mechanics*, Vol. 138, January 1984, pp.249-271.

[6] Tam, C.K.W., and Chen, P., "Turbulent Mixing Noise from Supersonic Jets," *AIAA Journal*, Vol. 32, No. 9, 1994, pp. 1774-1780.

[7] Dahl, M.D. and Morris, P.J., "Noise from Supersonic Coaxial Jets, Part 2: Normal Velocity Profile," *Journal of Sound and Vibration*, Vol. 200, No.5, 1997, pp. 665-699.

[8] Mitchell, B.E., Lele, S.K., and Moin, P., "Direct Computation of Mach Wave Radiation in an Axisymmetric Supersonic Jet," *AIAA Journal*, Vol. 35, No. 10, 1994, pp. 1574-1580.

[9] McLaughlin, D.K., Morrison, G.D., and Troutt, T.R., "Experiments on the Instability Waves in a Supersonic Jet and their Acoustic Radiation", *Journal of Fluid Mechanics*, Vol. 69, No. 11, 1975, pp.73-95.

[10] Seiner, J.M., Bhat, T.R.S, and Ponton, M.K., "Mach Wave Emission from a High-Temperature Supersonic Jet", *AIAA Journal*, Vol. 32, No. 12, 1994, pp. 2345-2350.

[11] Seiner, J.M., and Krejsa E., "Supersonic Jet Noise and the High Speed Civil Transport", AIAA-89-2358.

[12] Fenno, C.C., Bayliss, A., and Maestrello, L., "Interaction of Sound from Supersonic Jets with Nearby Structures," *AIAA Journal*, Vol. 36, No. 12, 1998, pp. 2153-2162.

[13] Hay, J.A. and Rose, E.G. "In-Flight Shock-Cell Noise," *Journal of Sound and Vibration,* Vol.11, 1970, pp. 411-420.

[14] Powell, A. "On the Mechanism of Choked Jet Noise," *Proceedings of the Physical Society, London*, Vol. 66, 1953, pp. 1039-1056.

[15] Tam, C.K.W, "Supersonic Jet Noise,", *Annual Review of Fluid Mechanics,* Vol. 27, 1995, pp. 17-43.

[16] Raman, G. "Advances in Understanding Supersonic Jet Screech," AIAA-98-0279.

[17] Papamoschou, D., Debiasi, M., "Noise Measurements in Supersonic Jets Treated with the Mach Wave Elimination Method," AIAA paper No. 98-0280, Jan. 1998; to appear in the *AIAA Journal.*

[18] Papamoschou. D., "Mach Wave Elimination from Supersonic Jets," *AIAA Journal*, Vol. 35, No. 10, 1997, pp. 1604-1611.

[19] Papamoschou, D. and Bunyajitradulya, A. "Evolution of Large Eddies in Compressible Shear Layers," *Physics of Fluids,* Vol. 4, No. 3, 1997, pp. 756-765.

[20] Murakami, E., and Papamoschou, D., "PLIF Investigation of Coannular Supersonic Jets," AIAA-98-3015.

[21] Tam, C.K.W, "Influence of Nozzle Geometry on the Noise of High-Speed Jets," *AIAA Journal*, Vol. 36, No. 8, 1997, pp. 1396-1400.

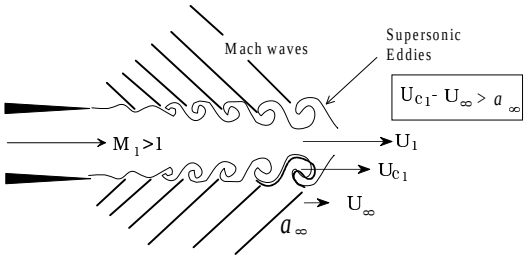

Figure 1: Mach wave radiation.

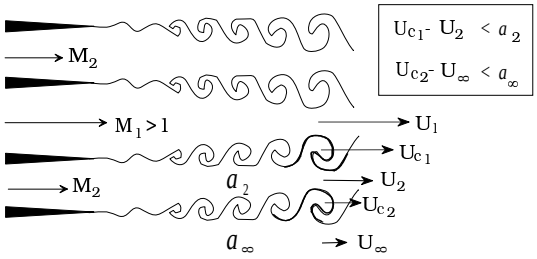

Figure 2: Principle of Mach wave elimination: creation of coflow adjacent to main jet so that all eddy motions become intrinsically subsonic.

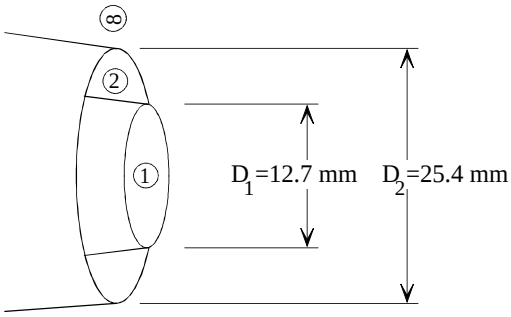

Figure 3: Coaxial nozzle arrangement.

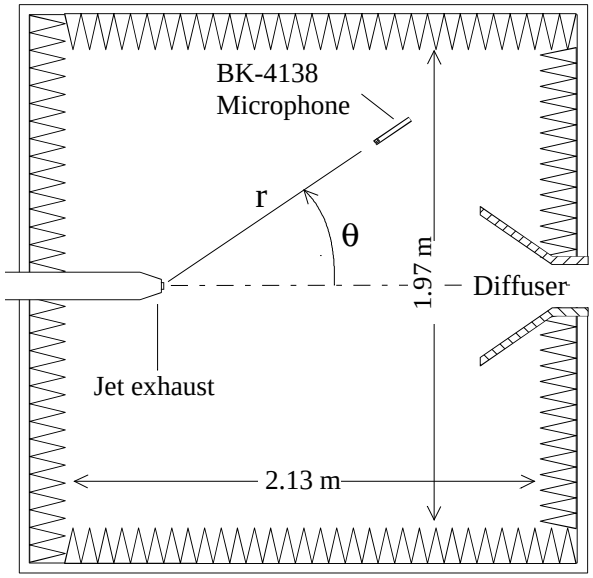

Figure 4: Anechoic chamber and positioning of jet and microphone.

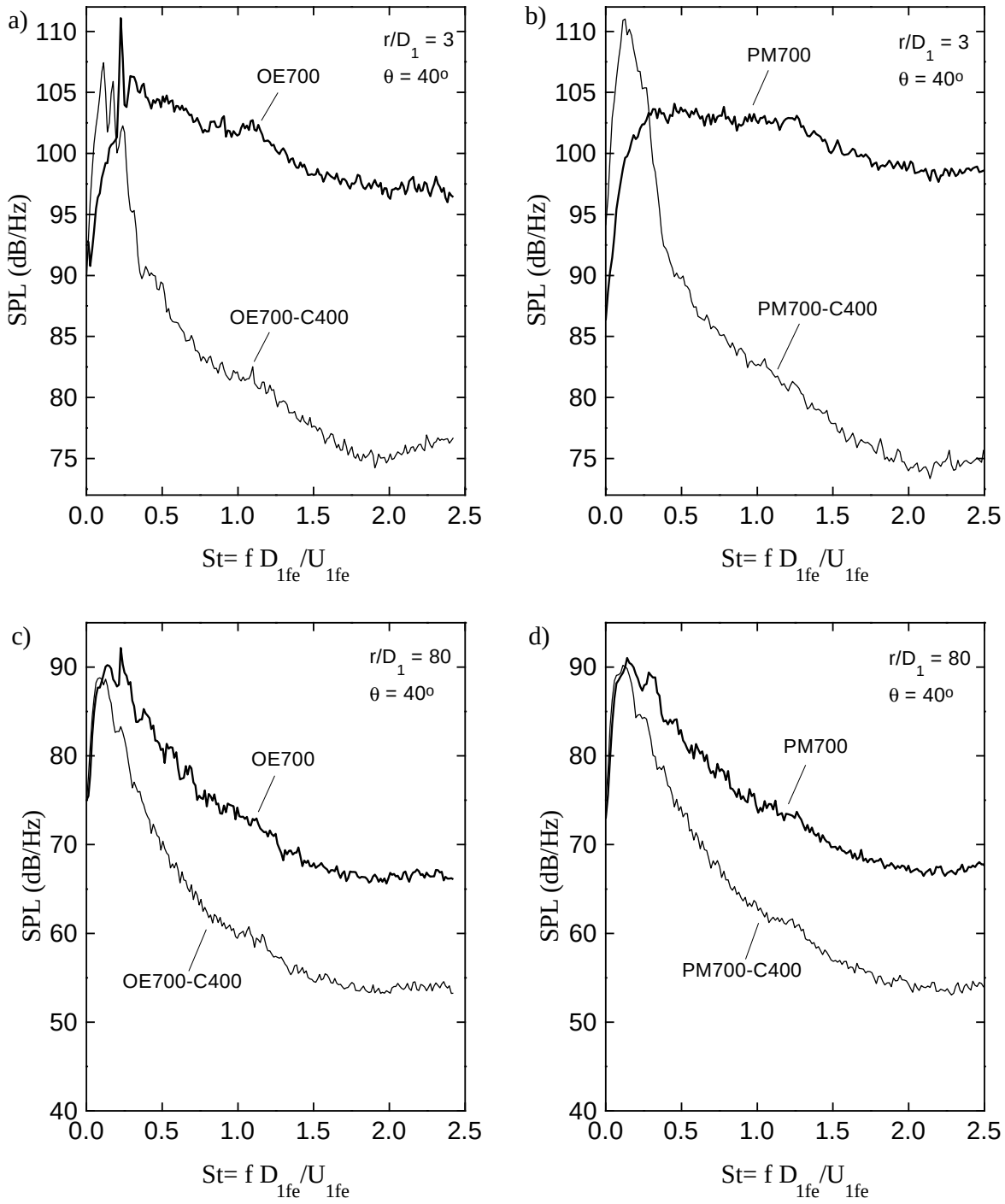

Figure 5: Effect of imperfect expansion on the peak noise emission of single and coaxial jets: comparison of over-expanded and pressure-matched jets at equal $U_{1\mathrm{fe}} = 700$ m/s and $M_{1\mathrm{fe}} = 1.5$. (a) OE700, $r/D_1 = 3$, $\theta = 40^o$; (b) PM700, $r/D_1 = 3$, $\theta = 40^o$; (c) OE700, $r/D_1 = 80$, $\theta = 40^o$; (d) PM700, $r/D_1 = 80$, $\theta = 40^o$.

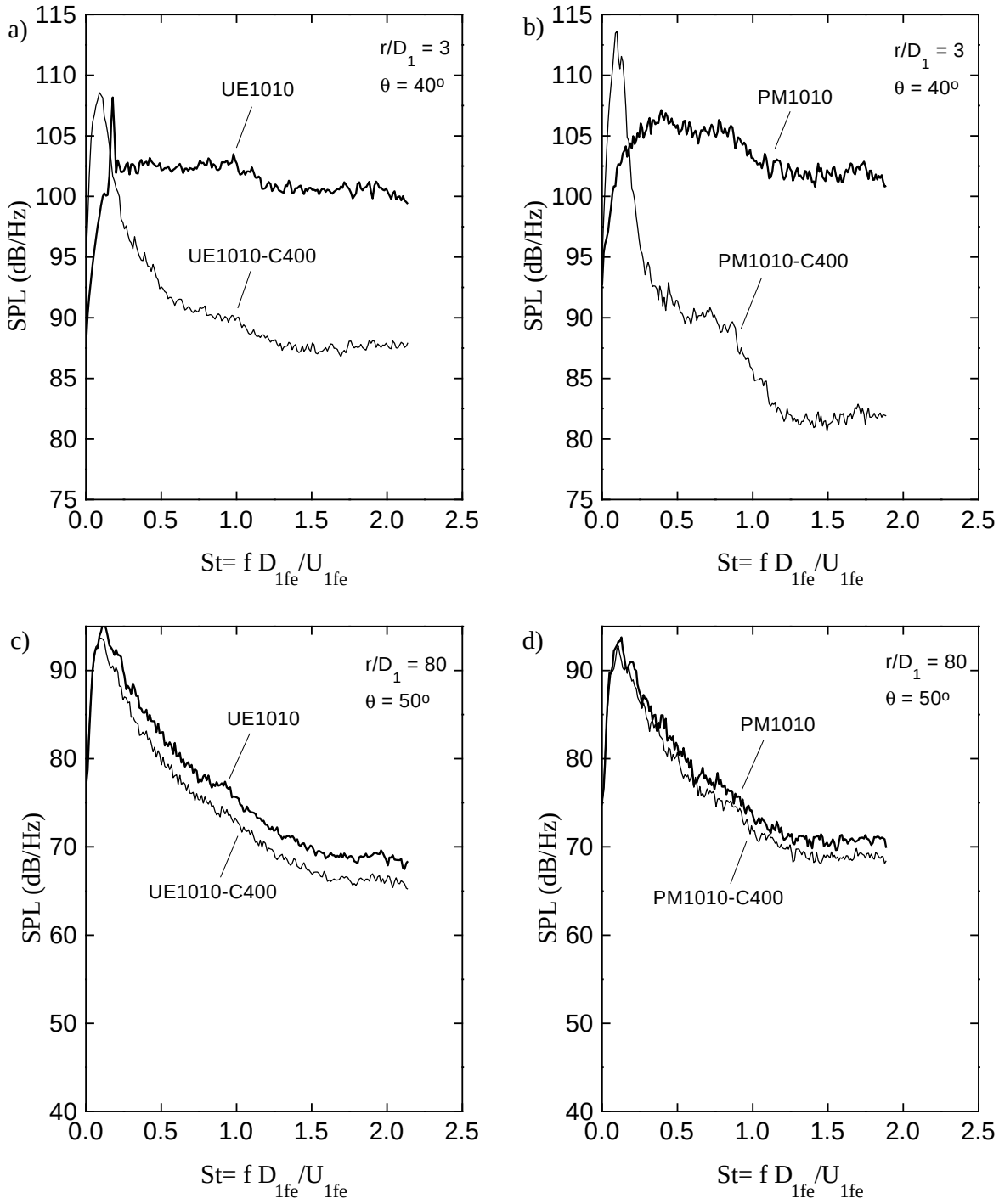

Figure 6: Effect of imperfect expansion on the peak noise emission of single and coaxial jets: comparison of under-expanded and pressure-matched jets at equal $U_{1\mathrm{fe}} = 1010$ m/s and $M_{1\mathrm{fe}} \approx 1.75$. (a) UE1010, $r/D_1 = 3$, $\theta = 40^o$; (b) PM1010, $r/D_1 = 3$, $\theta = 40^o$; (c) UE1010, $r/D_1 = 80$, $\theta = 50^o$; (d) PM1010, $r/D_1 = 80$, $\theta = 50^o$.

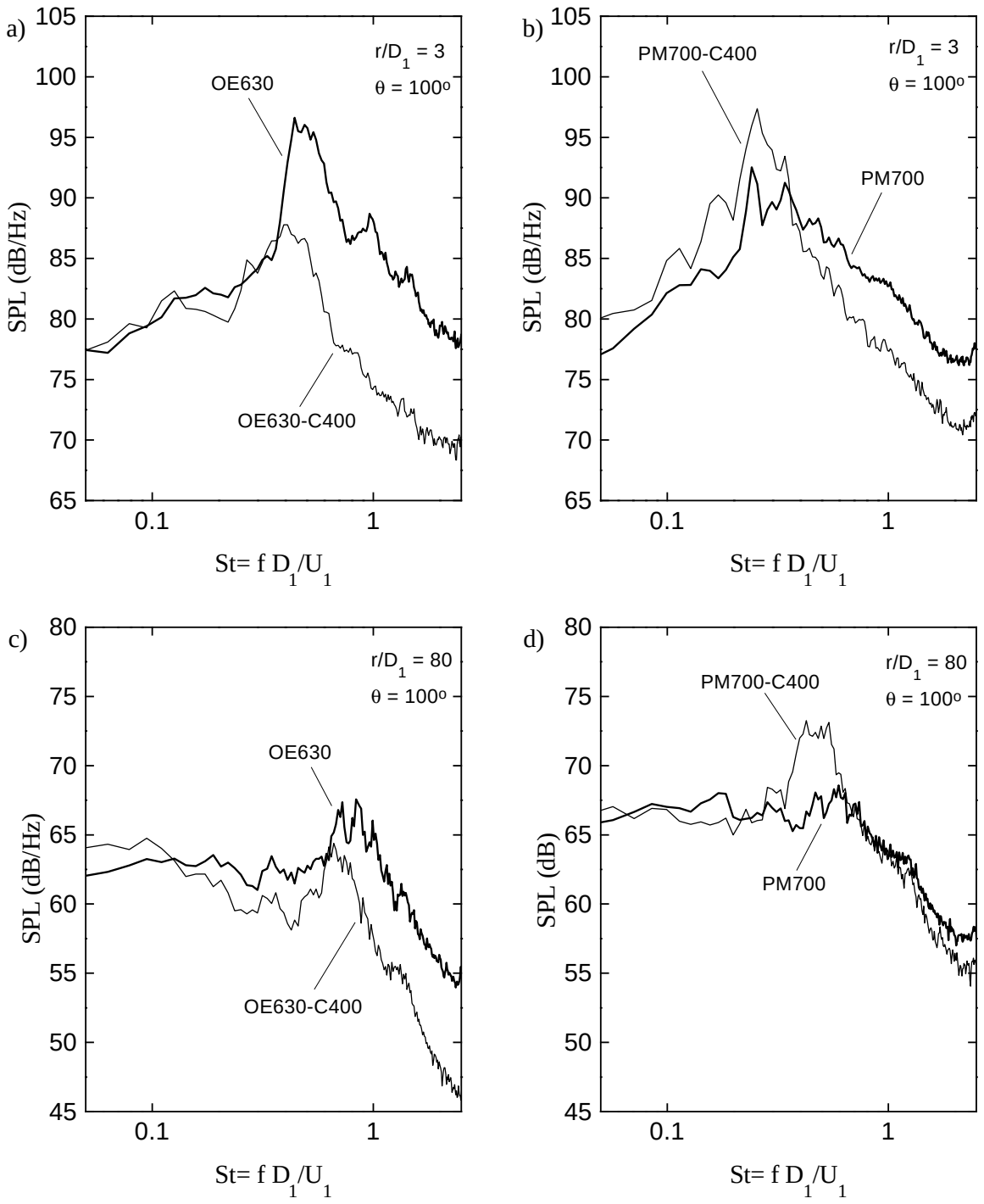

Figure 7: Effect of imperfect expansion on lateral noise emission in the direction $\theta = 100°$ for single and coaxial jets: comparison of over-expanded and pressure-matched jets at equal nozzle exit values $U_1 = 700$ m/s and $M_1 = 1.5$. (a) OE630, $r/D_1 = 3$; (b) PM700, $r/D_1 = 3$; (c) OE630, $r/D_1 = 80$; (d) PM700, $r/D_1 = 80$.

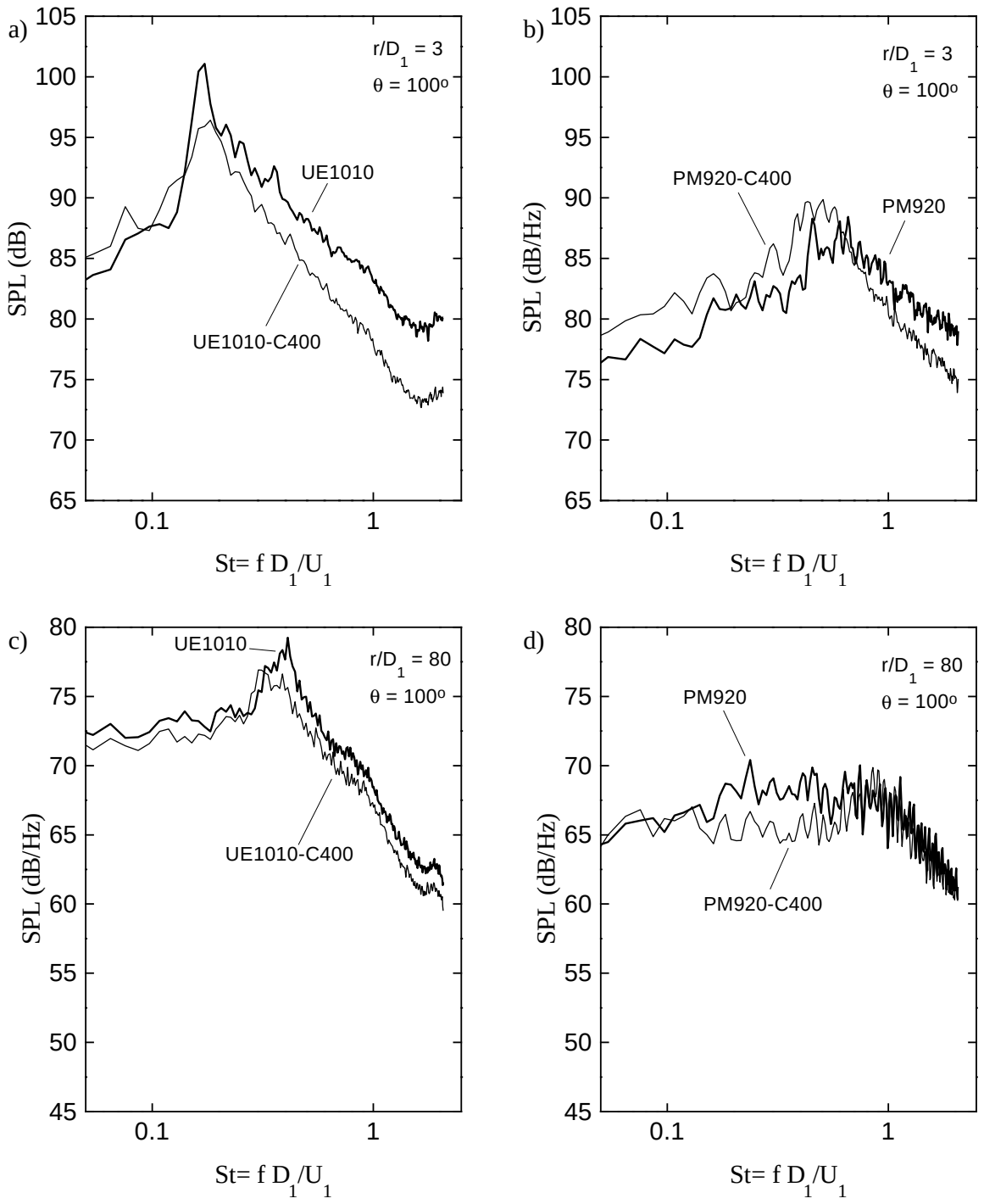

Figure 8: Effect of imperfect expansion on lateral noise emission in the direction $\theta = 100°$ for single and coaxial jets: comparison of under-expanded and pressure-matched jets at equal nozzle exit values $U_1 = 920$ m/s and $M_1 = 1.5$. (a) UE1010, $r/D_1 = 3$; (b) PM920, $r/D_1 = 3$; (c) UE1010, $r/D_1 = 80$; (d) PM920, $r/D_1 = 80$.

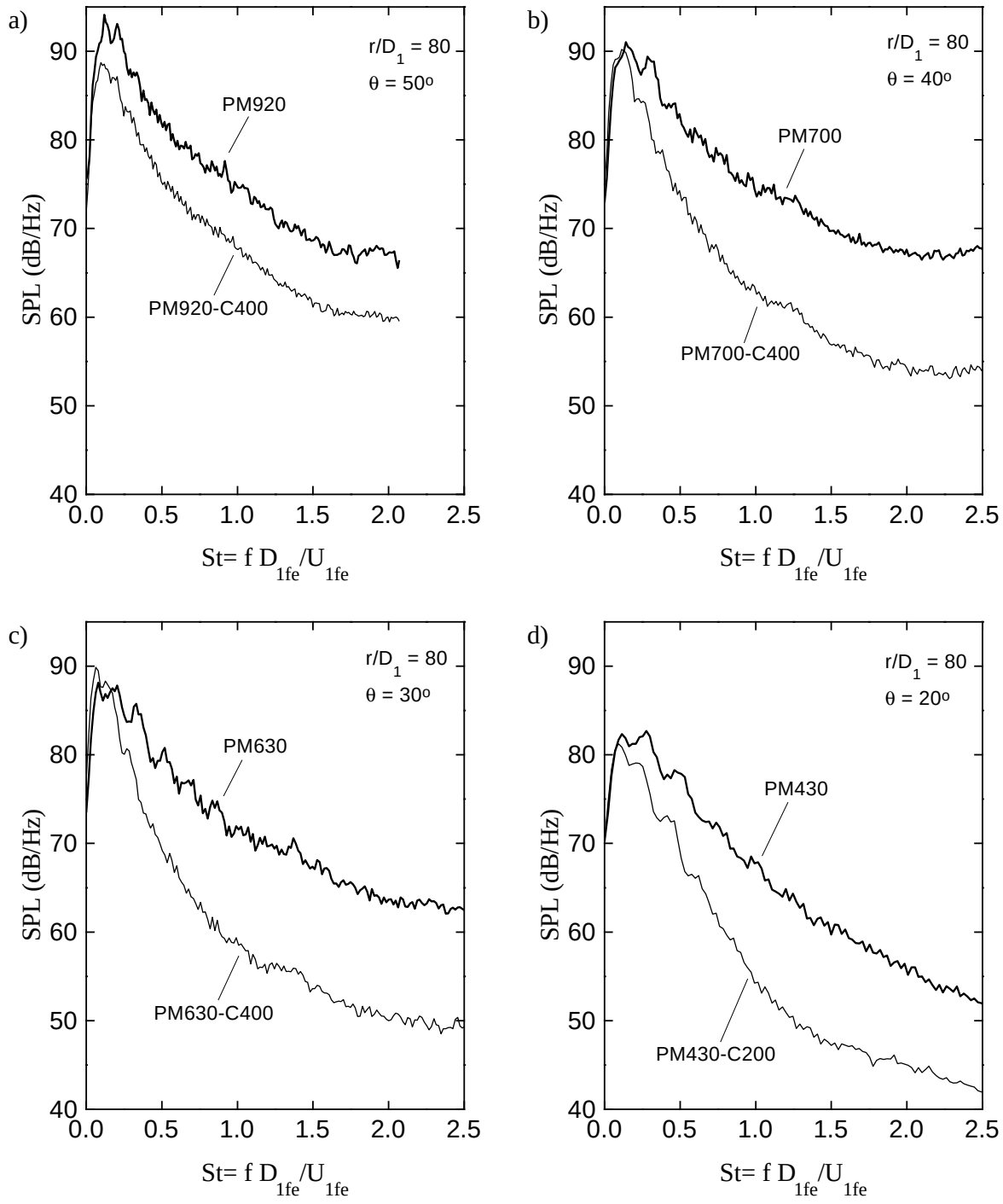

Figure 9: Effect of $U_{1\text{fe}}$ on far-field peak noise emission of single and coaxial jets with $M_{1\text{fe}} = 1.5$: (a) PM920, $\theta = 50^o$; (b) PM700, $\theta = 40^o$; (c) PM630, $\theta = 30^o$; (d) PM430, $\theta = 20^o$.

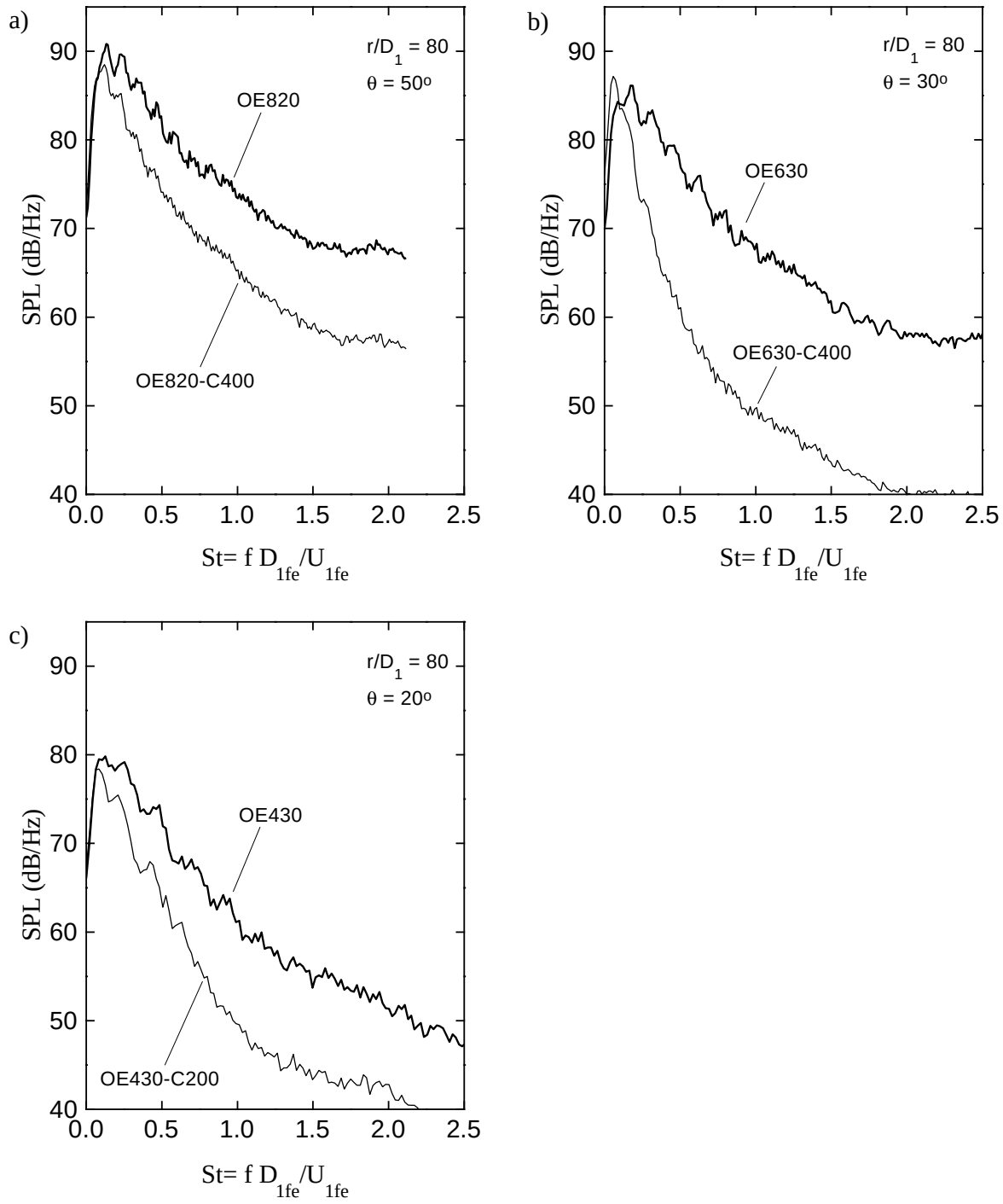

Figure 10: Effect of $U_{1\text{fe}}$ on far-field peak noise emission of single and coaxial jets with $M_{1\text{fe}} \approx 1.3$: (a) OE820, $\theta = 20^o$; (b) OE630, $\theta = 30^o$; (c) OE430, $\theta = 20^o$.

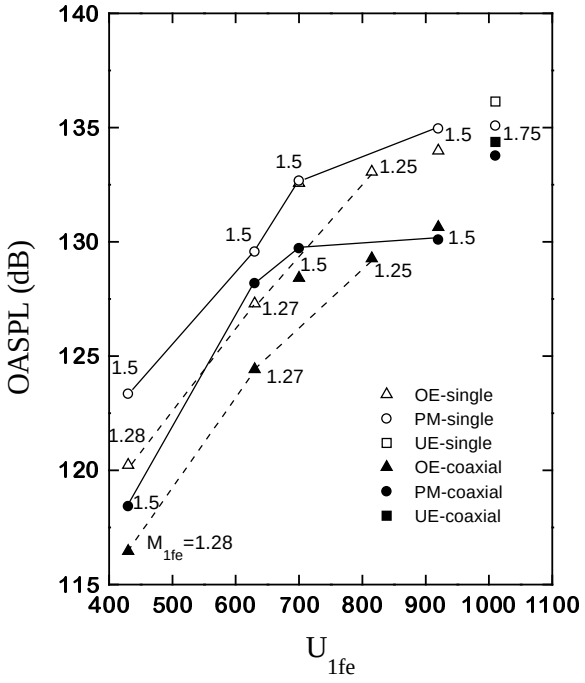

Figure 11: Effect of M_{1fe} and U_{1fe} on far-field OASPL in the direction of peak emission for single and coaxial jets. Solid lines connect data with $M_{1fe} = 1.5$, dashed lines connect data with $M_{1fe} \approx 1.3$.

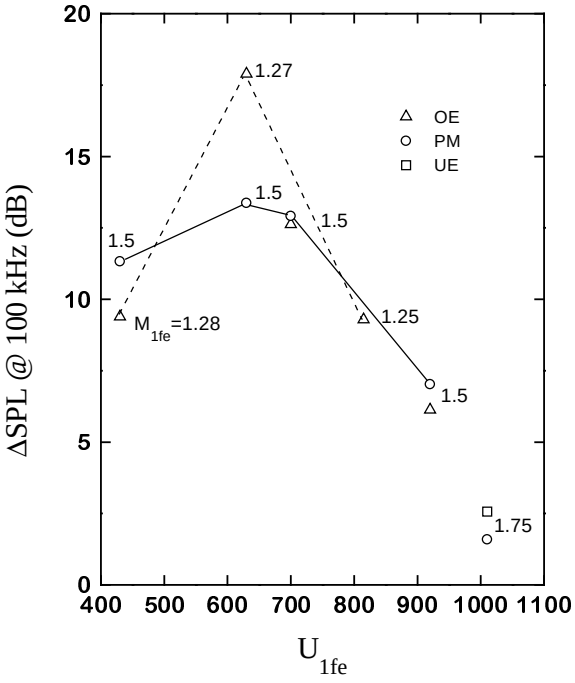

Figure 13: Reduction of far-field $\mathrm{SPL}_{100\text{-kHz}}$, in the direction of peak emission, resulting from application of the coflow. Solid lines connect data with $M_{1fe} = 1.5$, dashed lines connect data with $M_{1fe} \approx 1.3$.

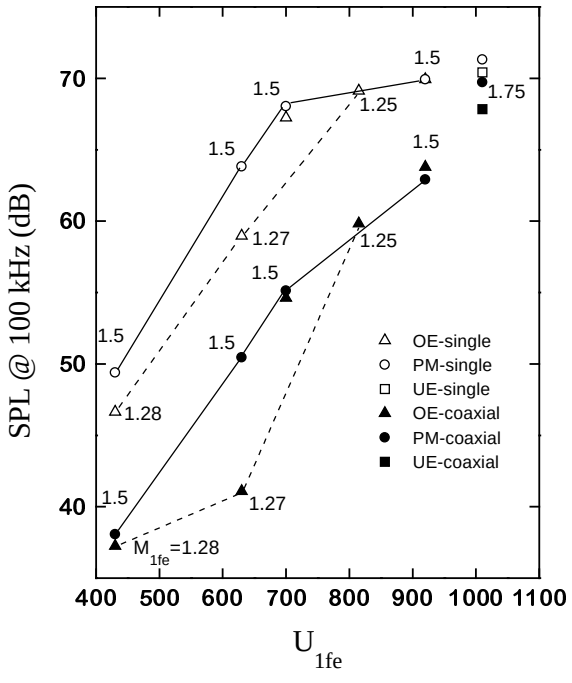

Figure 12: Effect of M_{1fe} and U_{1fe} on far-field $\mathrm{SPL}_{100\text{-kHz}}$ in the direction of peak emission for single and coaxial jets. Solid lines connect data with $M_{1fe} = 1.5$, dashed lines connect data with $M_{1fe} \approx 1.3$.